Journal of Magnetism and Magnetic Materials 322 (2010) 808–813

Contents lists available at ScienceDirect

Journal of Magnetism and Magnetic Materials

journal homepage: www.elsevier.com/locate/jmmm

Magnetic properties of iron-based soft magnetic composites with MgO coating obtained by sol–gel method

A.H. Taghvaei [a,*], A. Ebrahimi [a], M. Ghaffari [b], K. Janghorban [a]

[a] Department of Materials Science and Engineering, School of Engineering, Shiraz University, Shiraz, Iran
[b] School of Electrical Electronic Engineering, Nanyang Technological University, Nanyang Avenue, Singapore 639798, Singapore

ARTICLE INFO

Article history:
Received 29 July 2009
Received in revised form
5 November 2009
Available online 12 November 2009

Keywords:
Soft magnetic composite
Coercivity
Electrical resistivity
Eddy current loss

ABSTRACT

Soft magnetic composites with a thin MgO insulating layer were produced by a sol–gel method. Energy dispersive X-ray spectroscopy, X-ray analysis, Fourier transform infrared spectroscopy, density measurement and compositional maps confirmed that thin layers of MgO covered the iron powders. Coercivity measurement showed that the stress relaxation and reduction of hysteresis loss efficiently occurred at 600 °C. At this temperature, the phosphate insulation of commercial SOMALOY™ samples degrade and their electrical resistivity, magnetic permeability and operating frequency decreases noticeably. The results show that the MgO insulation has a greater heat resistance than conventional phosphate insulation, which enables stress-relief at higher temperatures (600 °C) without a large increase in eddy current loss. The results of annealing at 600 °C show that the electrical resistivity and ferromagnetic resonance frequency increased from 11 μΩ m and 1 kHz for SOMALOY™ samples to 145 μΩ m and 100 kHz for the MgO insulated composites produced in this work.

1. Introduction

In recent years, soft magnetic composites (SMCs) have been used in different applications. These materials have unique magnetic properties such as magnetic and thermal isotropy, very low eddy current loss and 3D magnetic properties in comparison with laminated steels [1–3]. SMCs are produced by compaction of insulated ferromagnetic powders such as high purity iron particles. One of the important challenging factors in the fabrication of SMCs is the considerable hysteresis loss at low frequencies due to internal stress. The compaction step imparts some cold work and residual stress in the particles and increases the dislocation density. This impedes the movement of domain walls and consequently increases the hysteresis loss.

Warm compaction can be used to eliminate the deleterious effects of residual stress and to improve soft magnetic properties [2]. Annealing treatment at high temperature is an effective method to decrease the internal strains and hysteresis loss. Generally, annealing can be imposed by three methods: thermal annealing, magnetic field annealing and thermal–magnetic field annealing [4]. Heat treatment reduces the distortion within particles, and as a result the coercive force reduces and the magnetic permeability increases [4]. However, the annealing temperature is limited by the thermal resistance of the insulating layer between the magnetic particles.

Phosphate insulation is commonly applied for conventional SMCs such as SOMALOY™ due to routine production and adhesiveness to iron powder [5–8], but has one shortcoming, the maximum annealing temperature, which is about 500 °C [9,10]. Therefore the stress-relief and reduction of hysteresis loss of phosphated powders cannot be completed at the typical stress-relief temperature for pure iron, which is between 570 and 775 °C [3]. Previously, the heat resistance and electrical resistivity of phosphated powders was improved by additional silane coating [10].

In the present work, a new kind of SMC with MgO insulation obtained by the sol–gel method was produced, and its magnetic properties measured and compared with the phosphated coated powders.

2. Experimental procedure

2.1. Materials

Iron powders with an average particle size $d < 150\ \mu m$ and a large size distribution were supplied by Merck. The purity of Fe was above 99% containing 0.02% C, 0.01% Cu, 0.005% Zn, 0.002% Pb and some oxides. Magnesium diethoxide $Mg(OEt)_2$ from Aldrich was the source of MgO coating on the iron particles, and SOMALOY™ powders purchased from Hoganas AB were used for comparison.

2.2. Preparation of MgO insulated powders by sol–gel method

Sol–gel method was used to create MgO insulation on the surface of iron powders. A proper amount of magnesium diethoxide (0.05 mole), deionized water (0.25 moles) and

* Corresponding author. Tel.: +98 711 8231756.
E-mail address: amirtaghvaei@gmail.com (A.H. Taghvaei).

0304-8853/$ - see front matter © 2009 Elsevier B.V. All rights reserved.
doi:10.1016/j.jmmm.2009.11.008

anhydrous ethanol (0.85 mole) were mixed with a constant stirring rate and kept for 10 min at room temperature. Then, 0.02 mole of ammonium hydroxide (pH=9) was added as a hydrolysis catalyst. The solution was kept under reflux condition at about 80 °C until gel formation was complete. The iron powders were mixed with 2.5 wt% gel in a spiral mixer. Mixing was carried out until total evaporation of solvent occurred. The coated powders were dried at 70 °C in air for 12 h and finally encapsulated in a quartz tube under argon atmosphere and heat treated at 600 °C for 4 h.

2.3. Composite production

The commercial SOMALOY™ and MgO insulated powders were compacted to 800 MPa in a toroid die with dimensions; outer diameter 13 mm, inner diameter 4 mm and height 2 mm. The compaction of samples was performed using graphite as the die wall lubricant. Finally, the produced composites were annealed in air at 400, 450, 500, 550, 600 and 650 °C for 30 min. For comparison, green compacts (without annealing) prepared from SOMALOY™, MgO insulated powders and uncoated powders were prepared and their magnetic properties were measured.

2.4. Characterization

MgO insulating layer was characterized by scanning electron microscopy (SEM JEOL-JSM-53101) coupled with energy dispersive spectrometer (EDS) and X-ray diffraction (XRD, Shimadzu 6000 using CuKα radiation). Coverage of particles with MgO coating was studied by elemental mapping to show the distribution of iron, oxygen and magnesium. To investigate the stability of MgO insulation after heat treatment, a cross-section of an annealed cylindrical specimen was provided using a suitable cutting tool. After polishing, the surface compositional maps of oxygen and magnesium were created by SEM image mapping. The effect of heat treatment on the composition of the sol–gel derived insulated powders was investigated using Fourier transform infrared spectrometer (FTIR, Shimadzu 8000). KBr pellet containing the particles was used for the FTIR spectroscopic measurements and the spectra were collected in a scan range between 500 and 4000 cm^{-1}. To study the effect of annealing treatment on the composition of the phosphating layer of SOMALOY™ powders, these powders were first encapsulated in a quartz tube under inert atmosphere and annealed at 600 °C for 30 min and then characterized by FTIR. Internal microstrain of the samples was calculated using the Williamson–Hall method [11]. Complex permeability of the toroid samples were measured by an impedance analyzer (HEWLETT PACKARD, 4195A, 10 Hz–500 MHz) at low flux densities. Loss factor was measured from R_s/L, where R_s is the sum of resistivity of winding and core, and L is the inductance of the core [12]. The coercivity of the samples was measured by a B–H curve analyzer (Magnet physics C-330). Electrical resistivity measurement was performed by use of four point probe method according to ASTMD4496-87 standard. Density of each sample was measured three times by the principle of Archimedes.

3. Result and discussion

3.1. Characterization of insulating layer

Fig. 1 depicts the EDS analysis of insulated powders after heating at a temperature of 600 °C for 4 h which consists of magnesium, oxygen and iron peaks. With respect to the analyzed depth, the comparison between the intensity of magnesium, oxygen and under laying iron peaks reveals that the insulating layer is thin. Fig. 2 represents the X-ray diffraction pattern of the coated powders after heating. The peak of low intensity (near 43°) may be attributed to the (2 0 0) plane of the MgO layer [13]. From the pattern, no impurity or other phases such as iron oxides were observed. The small intensity of the crystalline MgO layer in the X-ray pattern, as well as the low intensity of Mg and O atoms in the EDS analysis confirms that the insulating layer is thin. The small thickness of the MgO layer had no noticeable effect on the compressibility of the iron powders. Thin insulation leads to the densities of the MgO insulated samples and uncoated compacts to be close to each other (Table 1). Also, the nature of the insulating layer can be assessed by FTIR analysis. Fig. 3a shows the FTIR spectra of coated iron powders before the final heating. It has been proposed that the preparation of metal oxides by sol–gel methods leads to highly hydroxylated materials, hence the band around 3600 cm^{-1} can be assigned to hydrogen bounded hydroxyl groups and $Mg(OH)_2$[12]. The Mg–O absorption peaks are expected in the 400–600 cm^{-1} region [13]. The small peak seen at 533 cm^{-1} is associated with the longitudinal optical (LO) phonon modes of the MgO lattice [13]. This implies that the insulation layer consists of MgO with some concentration of hydroxide. After heating at 600 °C, the intensity of the peak corresponding to the hydroxyl groups at 3600 cm^{-1} decreased

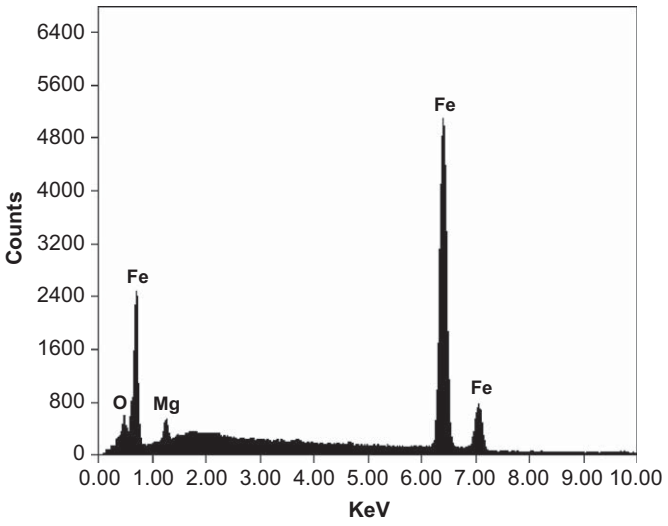

Fig. 1. EDS analysis of MgO insulated powders after heating at 600 °C for 4 h.

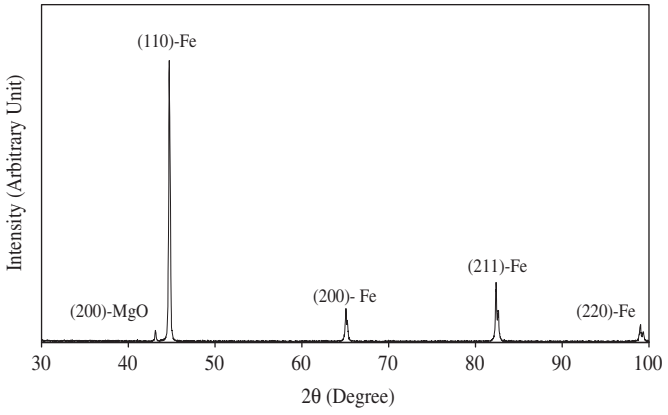

Fig. 2. XRD of MgO insulated powders after heating at 600 °C for 4 h.

and the Mg–O absorption intensity increased. These effects arise from the large thermal conversion of magnesium hydroxide to magnesium oxide (Fig. 3b). From this figure, it can be concluded that the sol–gel process successfully created the MgO layer on the surface of the iron particles.

Table 1
Measured density for uncoated and MgO insulated compacts.

Compaction pressure (MPa)	MgO insulated samples density (g/cm^3)	Uncoated samples density (g/cm^3)
600	6.89	6.92
800	7.29	7.31
1200	7.70	7.72

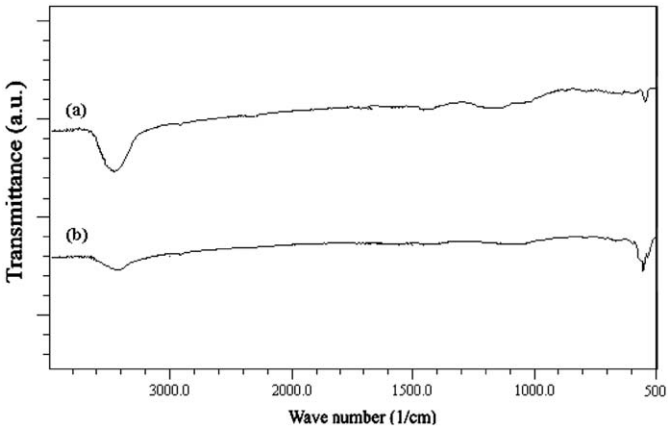

Fig. 3. FTIR spectra of iron powders after sol–gel process (a) before heating and (b) after heating at 600 °C for 4 h.

Coverage of iron the powders surface with the MgO layer is confirmed by the X-ray maps of oxygen and magnesium distributions for the selected areas of powders (Fig. 4). It is clear that the sol–gel process resulted in a uniform coverage of the surface of the powders by the insulating layer.

3.2. Magnetic properties

Fig. 5 shows the permeability of the uncoated samples and green MgO insulated compacts at different frequencies. At very low frequencies, the difference in the real part of permeability in the two samples is negligible. Thin insulation, which was previously characterized, means less distributed air gaps and higher magnetic permeability at low frequencies. At higher frequencies, thin MgO insulation decreases the inter particle connections and eddy currents in the samples by confining them in the particles. Fewer eddy currents increase the frequency stability, penetration depth of flux density and magnetic permeability at high frequencies.

Fig. 6 shows the dependence of coercivity of phosphated and MgO insulated compacts with the annealing temperature. Annealing decreases the coercivity by decreasing the internal microstrain and strain anisotropy [3]. Data in Table 2 predicted that increasing the annealing temperature would decrease the microstrain and consequently the coercivity. From Fig. 6, the sample coercivity decreased linearly with increasing the annealing temperature from 400 to 600 °C and it became almost constant at 600 °C. This means that 600 °C is high enough as an annealing temperature for stress-relief of the samples to decrease the coercivity and consequently the hysteresis loss.

Fig. 7 shows the effect of annealing treatment at different temperatures on the real part of magnetic permeability of phosphated compacts. The compaction step is believed to always create some plastic deformation in the powders, which consequently increases the dislocation density in the particles.

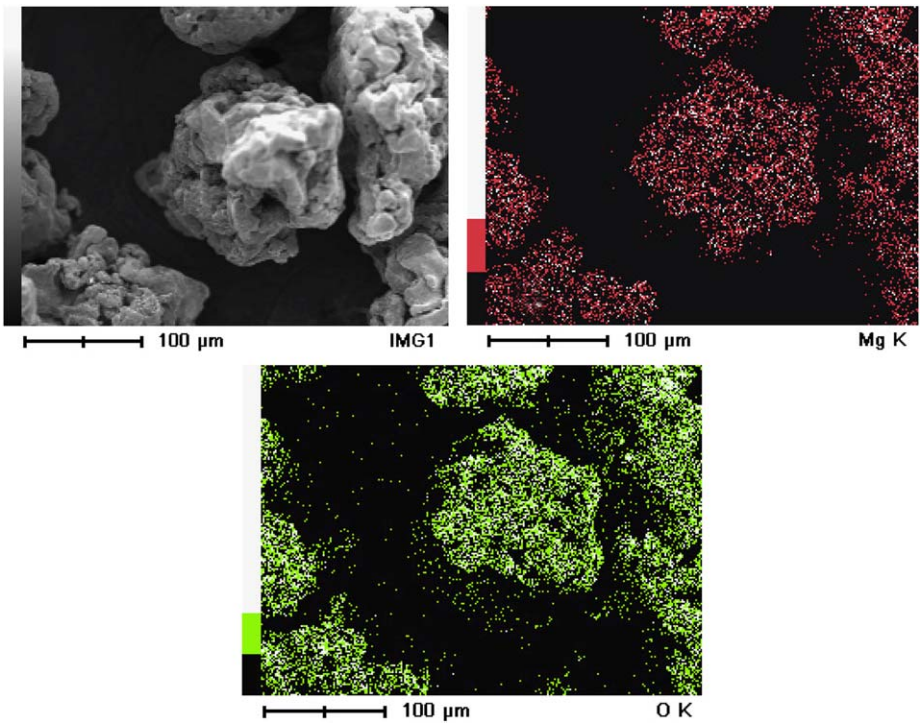

Fig. 4. Maps of oxygen and magnesium of MgO insulated iron powders.

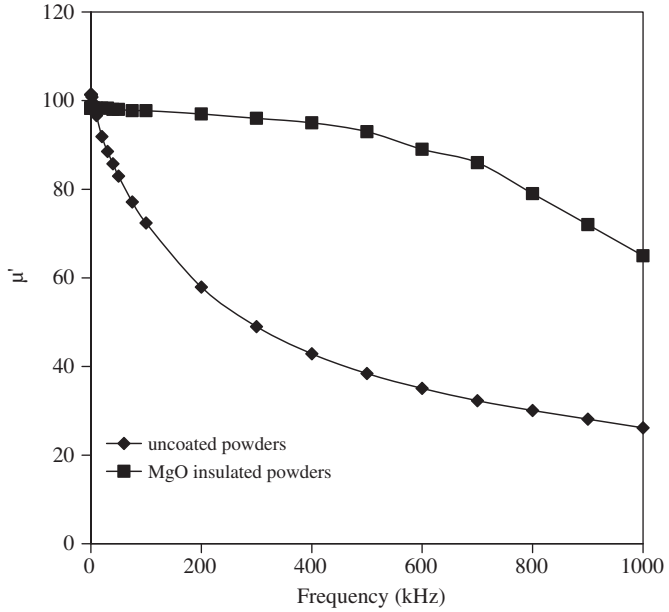

Fig. 5. Variation of real part of permeability for uncoated and green MgO insulated compacts with frequency.

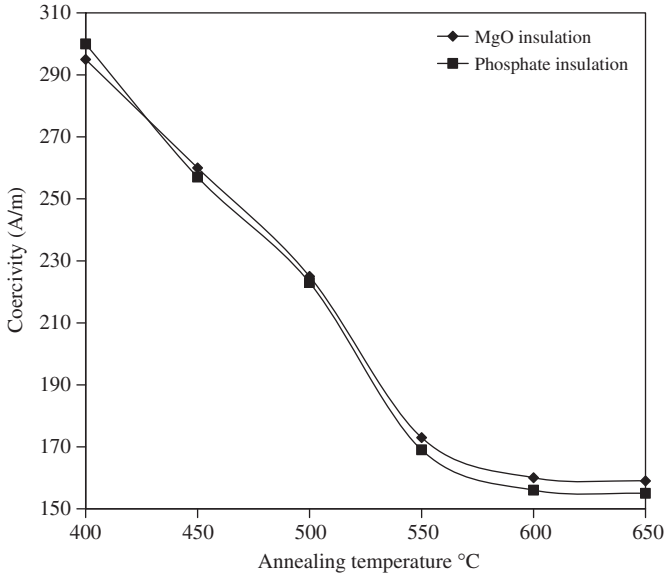

Fig. 6. Effect of annealing temperature on the coercivity of phosphated and MgO insulated compacts.

Table 2
Effect of annealing temperature on the internal microstarin of compacts.

Microstrain (%)	Annealing temperature (°C)
0.43	Without annealing
0.38	400
0.28	500
0.13	550
0.10	600
0.09	650

Dislocations act as pinning centers and impede the movement of the magnetic domain walls. Heat treatment reduces the distortion within the particles, lowers dislocation density, and hence increases the magnetic permeability [4]. The reduction of residual stress and the increase of the magnetic permeability is larger at higher temperatures. As mentioned before, stress relaxation and decrease in coercivity is significant at annealing temperatures about 600 °C, but this temperature strongly decreases the real part of permeability. Even at low frequencies, this reduction results from degradation of the phosphating layer and the increase in eddy currents [10]. Fig. 8 depicts the FTIR spectra of the phosphated powders before annealing (a) and after annealing at 600 °C (b). According to this figure, the band near 1100 cm^{-1}, which indicates the PO_4^{3-} vibration [14,15], disappears after annealing. The phosphate insulation may be degraded due to the mutual diffusion of iron, phosphorus and oxygen through the phosphate coating [10]. The phosphate degradation severely decreases the electrical resistivity and then increases the imaginary part of permeability (Fig. 9). Annealing of phosphate compacts decreases the ferromagnetic resonance frequency (f_r) according to the following equation [16]:

$$f_r = \rho/2\pi\mu_0\mu_i d^2 \quad (1)$$

where ρ is the specific electrical resistivity, μ_0 is the magnetic constant, μ_i is the initial permeability and d is the diameter of the particles [16]. From Fig. 9, annealing at 600 °C decreased f_r to about 1 kHz.

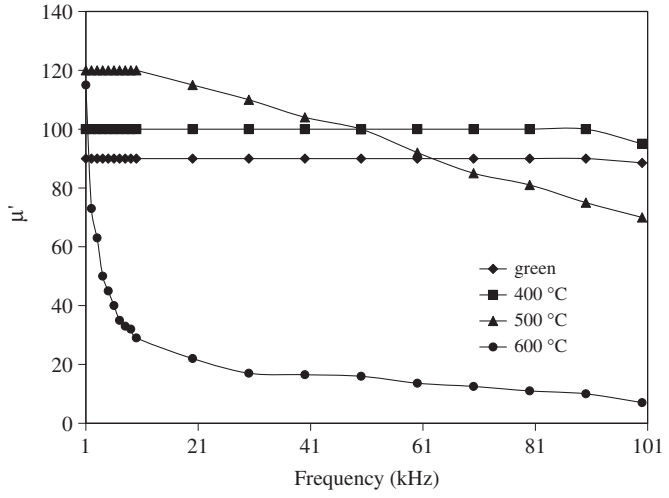

Fig. 7. Effect of annealing temperature on the real part of permeability of phosphated compacts at different frequencies.

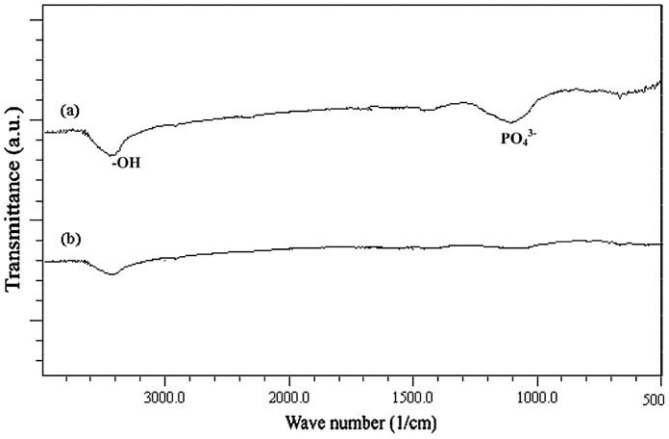

Fig. 8. FTIR spectra of the phosphated powders (a) before annealing and (b) after annealing at 600 °C.

Table 3 shows the effect of annealing temperature on the electrical resistivity of phosphated and MgO insulated compacts. As a general trend electrical resistivity decreased with increasing the annealing temperature. The resistivity of the samples with phosphate insulation dropped to 4 μΩ m at 650 °C due to phosphate degradation, but the values of resistivity for the MgO insulated samples are noticeably greater than the phosphated compacts at each annealing temperature. As shown in Fig. 3b, the band around 533 cm^{-1} which corresponds to MgO absorption remained after annealing at 600 °C and no degradation of insulation occurred. Fig. 10 illustrates the maps of magnesium and oxygen at the cross-section of the MgO insulated compacts after annealing at 600 °C. This figure shows that magnesium and oxygen were distributed homogenously along the particles boundary. As a result, the continuous MgO insulation remains along the particle boundaries after annealing, therefore the MgO insulation has superior heat resistance to phosphate insulation coating and its structural continuity is preserved, even after annealing at 600 °C.

Fig. 11 shows the loss factor of the phosphated and MgO insulated samples annealed at 600 °C at different frequencies. By approximation, the loss factor can be replaced by eddy current loss factor at high frequencies, which has the following relationship with electrical resistivity [12]:

$$\frac{\tan\delta}{\mu} = \frac{\pi f \mu_0 D^2}{\rho \beta} \tag{2}$$

where μ is the permeability, μ_0 is a magnetic constant, f is the frequency, D is diameter of the material, tan δ is the eddy current loss factor, β is the shape factor and ρ is the specific resistivity [12]. From the previous discussion and Eq. (2), the high electrical resistivity of MgO insulated compacts, even after annealing at 600 °C decreased the eddy current loss factor. Also, the ferromagnetic resonance frequency increased from 1 kHz for phosphated powders to above 100 kHz for MgO insulated compacts. (Fig. 12). Decrease in eddy current in the MgO insulated sample, suppresses their demagnetizing field and increases the frequency stability and real part of permeability in comparison with the phosphated compacts (Fig. 13).

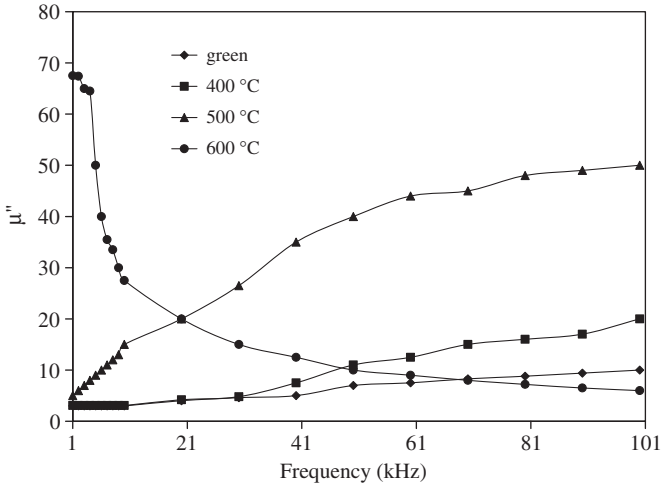

Fig. 9. Effect of annealing temperature on the imaginary part of permeability of phosphated compacts at different frequencies.

Table 3
Effect on annealing temperature on the electrical resistivity of phosphated and MgO insulated compacts.

Annealing temperature (°C)	Resistivity (μΩ m) phosphate	Resistivity (μΩ m) MgO
400	75	325
450	70	305
500	45	270
550	14	200
600	11	145
650	4	85

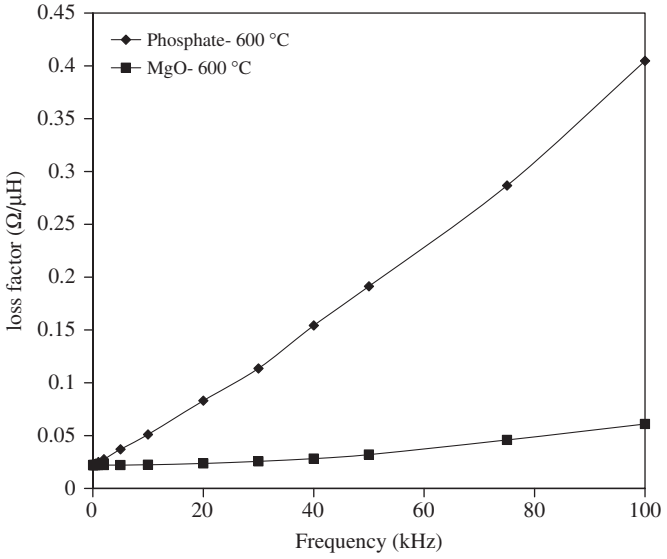

Fig. 11. Variation of loss factor with frequency for phosphated and MgO insulated compacts annealed at 600 °C.

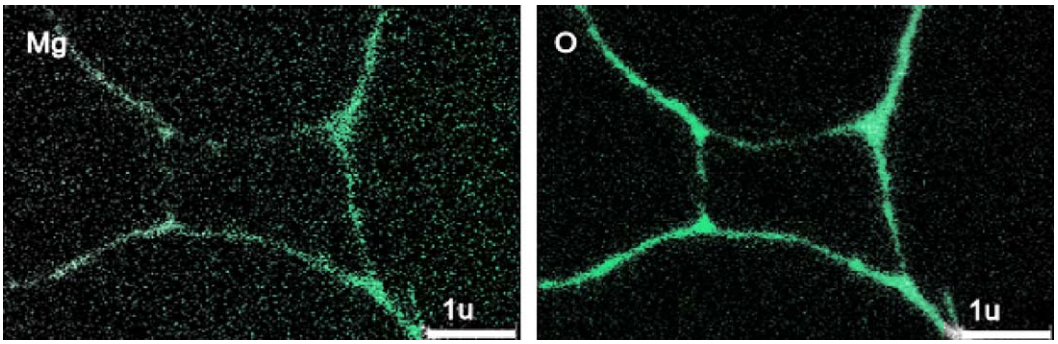

Fig. 10. Maps of magnesium and oxygen at cross-section of the MgO insulated compacts annealed at 600 °C.

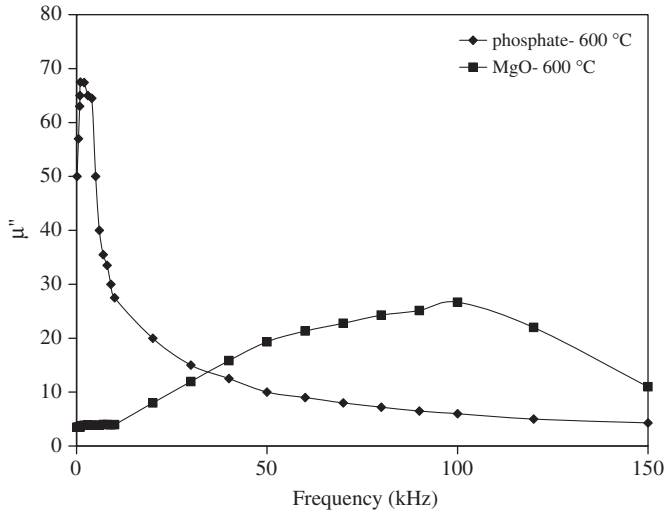

Fig. 12. Variation of imaginary part of permeability with frequency for phosphated and MgO insulated compacts annealed at 600 °C.

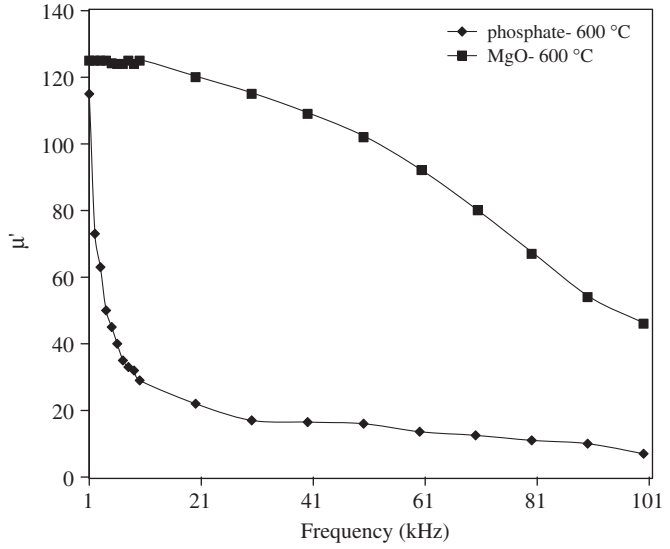

Fig. 13. Variation of real part of permeability with frequency for phosphated and MgO insulated compacts annealed at 600 °C.

4. Conclusions

The following conclusions could be drawn from this work:

(1) EDS and X-ray analysis, FTIR spectra and density measurements showed that the particles surface layer contained a thin MgO insulating layer with uniform coverage of the powder surfaces after sol–gel processing.

(2) Measurement of the internal strains and coercivity revealed that significant stress relaxation, minimum coercivity and hysteresis loss occurred after annealing at 600 °C for both phosphated and MgO insulated compacts.

(3) The MgO insulation had greater thermal stability with respect to the phosphate insulation coating of SOMALOY™ powders and its structural continuity was preserved even after annealing at 600 °C.

(4) The SMCs with MgO insulation had lower eddy current loss, higher electrical resistivity, ferromagnetic resonance frequency, frequency stability and magnetic permeability after annealing at 600 °C with respect to the phosphated compacts.

References

[1] H. Shokrollahi, K. Janghorban, Soft magnetic composites, J. Mater. Process. Technol. 189 (2007) 1–12.
[2] H. Shokrollahi, K. Janghorban, Effect of warm compaction on magnetic and electrical properties of Fe-based soft magnetic composite, J. Magn. Magn. Mater. 313 (2007) 182–186.
[3] H.R. Hemmati, H. Madaah Hosseini, A. Kianvash, The correlations between processing parameters and magnetic properties of an iron–resin soft magnetic composite, J. Magn. Magn. Mater. 305 (2006) 147–151.
[4] H. Shokrollahi, K. Janghorban, Different annealing treatments for improvement of magnetic and electrical properties of soft magnetic composites, J. Magn. Magn. Mater. 313 (2007) 182–186.
[5] J.J. Zhong, J.G. Zhu, Z.W. Lin, Y.G. Guo, J.D. Sievert, Improved measurement of magnetic properties with 3D magnetic fluxes, J. Magn. Magn. Mater. 290 (2005) 1567–1570.
[6] J.J. Zhong, Y.G. Guo, J.G. Zhu, Z.W. Lin, Characteristics of soft magnetic composite material under rotating magnetic fluxes, J. Magn. Magn. Mater. 299 (2006) 29–34.
[7] S. Gimenez, T. Lauwagie, G. Roebben, W. Heylen, O. Van der Biest, Effects of microstructural heterogeneity on the mechanical properties of pressed soft magnetic composite bodies, J. Alloys Compd. 419 (2006) 299–305.
[8] Z.W. Lin, J.G. Zhu, Three-dimensional magnetic properties of soft magnetic-composite materials, J. Magn. Magn. Mater. 299 (2006) 29–34.
[9] T. Madea, H. Toyoda, N. Igarashi, K. Hirose, K. Mimura, T. Nishikoa, A. Ikejaya, Development of super low iron-loss P/M soft magnetic material, SEI Tech. Rev. 60 (2005) 3–9.
[10] A.H. Taghvaei, H. Shokrollahi, K. Janghorban, Properties of iron-based soft magnetic composite with iron phosphate–silane insulation coating, J. Alloys Compd. 481 (2009) 681–686.
[11] G.K. Williamson, W.H. Hall, X-ray line broadening from filed aluminum and wolfram, Acta Metall. 1 (1953) 22–31.
[12] E.C. Snelling, Ferrites for Inductors and Transformers, Research Studies Press, Letchworth, New York, 1983.
[13] A. Moses, L.C. Nehru, M. Jayachandran, C. Sanjeeviraja, Spray pyrolysis deposition and characterization of highly (1 0 0) oriented magnesium oxide thin films, Cryst. Res. Technol. 42 (2007) 867–875.
[14] N. Colthup, H. Lawrence, S.E..Wiberley, Introduction to Infrared and Raman Spectroscopy, second ed. New york, 1964.
[15] H. Monma, Electrolytic depositions of calcium phosphates on substrate 29 (1994) 949–953J. Mater. Sci. 29 (1994) 949–953.
[16] R..Barrue, F..Mazaleyrat, Soft magnetic amorphous and nanocrystalline magnetic materials, in: H.S. Nalwa (Ed.), Handbook of Advanced Electronic and Photonic Materials and Devices, 2001.